[redacted]

Copy 133
RM H55A13

NACA RM H55A13

RESEARCH MEMORANDUM

FLIGHT EXPERIENCE WITH TWO HIGH-SPEED AIRPLANES HAVING VIOLENT LATERAL-LONGITUDINAL COUPLING IN AILERON ROLLS

By NACA High-Speed Flight Station

High-Speed Flight Station
Edwards, Calif.

CLASSIFICATION CHANGED
TO Unclassified
BY AUTHORITY OF RA #129 Date 17 July 1958
SFD, 18 Jul 1963

CLASSIFIED DOCUMENT

This material contains information affecting the National Defense of the United States within the meaning of the espionage laws, Title 18, U.S.C., Secs. 793 and 794, the transmission or revelation of which in any manner to an unauthorized person is prohibited by law.

NATIONAL ADVISORY COMMITTEE FOR AERONAUTICS

WASHINGTON

February 4, 1955

[redacted]

NATIONAL ADVISORY COMMITTEE FOR AERONAUTICS

RESEARCH MEMORANDUM

FLIGHT EXPERIENCE WITH TWO HIGH-SPEED AIRPLANES HAVING VIOLENT LATERAL-LONGITUDINAL COUPLING IN AILERON ROLLS

By NACA High-Speed Flight Station

SUMMARY

During flight tests of two high-speed airplane configurations, violent cross-coupled lateral and longitudinal motions were encountered following abrupt rudder-fixed aileron rolls. The speeds involved ranged from a Mach number of 0.7 to 1.05. The motions were characterized by extreme variations in angles of attack and sideslip which resulted in load factors as large as 6.7g (negative) and 7g (positive) normal acceleration and 2g transverse acceleration.

INTRODUCTION

During flight testing of the X-3 straight-wing research airplane and a swept-wing fighter-type airplane, a number of aileron maneuvers were performed which resulted in extremely violent inadvertent lateral and longitudinal motions. In the case of the X-3 the inadvertent motions resulted from level-flight aileron rolls at $M = 0.92$ and 1.05. The fighter airplane encountered the violent motions as a result of an aileron roll at $M = 0.70$. In all cases the motions were characterized by the attainment of large angles of sideslip and attack with resulting high load factors.

The present paper presents the first data with little attempt at analysis, since it is felt that data showing this behavior will be of general interest in that other current airplanes might be expected to encounter similar behavior.

SYMBOLS

A_Y	transverse acceleration at center of gravity, g units
A_Z	normal acceleration, g units
BM	structural bending-moment load, exposed panel, in.-lb
C_{N_A}	airplane normal-force coefficient, $A_Z W/qS$
F_a	aileron stick force, lb
F_r	rudder pedal force, lb
F_s	elevator stick force, lb
h_p	pressure altitude, ft
i_t	incidence angle of all movable tail, leading edge up is positive, deg
L	structural shear load, exposed panel, lb
M'	Mach number, corrected for level-flight position error
$M_{c/4}$	structural torque load, exposed panel about the quarter-chord of the panel mean aerodynamic chord, in.-lb
P	static pressure, lb/sq ft
p	rolling angular velocity, radians/sec
$\dot{p}$	rolling angular acceleration, radians/sec^2
q	pitching angular velocity, radians/sec
q	dynamic pressure, $0.7\ M^2P$
$\dot{q}$	pitching angular acceleration, radians/sec^2
r	yawing angular velocity, radians/sec
$\dot{r}$	yawing angular acceleration, radians/sec^2
S	wing area, sq ft

t	time, sec
W	airplane weight, lb
α	indicated angle of attack, deg
β	indicated angle of sideslip, deg
δ_a	aileron angle, deg
δ_r	rudder angle, deg

Subscripts:

W	wing
HT	horizontal tail
VT	vertical tail

AIRPLANES AND INSTRUMENTATION

The mass and geometric characteristics of airplane A, the X-3 research airplane, are presented in table I, a three-view drawing is shown as figure 1, and photographs are shown as figure 2.

Airplane B is a fighter type, the mass and geometric characteristics of which are presented in table II. A three-view drawing is shown as figure 3 and photographs as figure 4.

Both of the airplanes were instrumented to record those quantities required for stability and control and wing and tail load investigations. The loads were measured by means of strain gages located at the root stations of the surfaces of airplane A and airplane B.

The Mach numbers presented are corrected by the airspeed calibration obtained in level flight for airplane A and from the manufacturer's calibration for airplane B.

TEST, RESULTS, AND DISCUSSION

The aileron maneuvers presented in this paper were performed during investigations of handling qualities and wing and tail structural and

aerodynamic loads and consisted of abrupt aileron rolls with rudder fixed performed from a wings level attitude.

The time history of an abrupt left aileron roll for airplane A flying at a Mach number of about 0.92 at an altitude of 30,000 feet is presented as figure 5. While the ailerons are deflected for the aileron roll, a favorable sideslip angle is generated, together with a rather large increase in angle of attack. (The initial decrease in angle of attack is probably attributable to pilot stabilizer control input.) At time 3.8 seconds, even though the pilot is now applying 10° right aileron control, left rolling velocity increased and exceeded 5 radians/sec accompanied by violent pitching and sideslipping motions. During this uncontrollable phase of the maneuver, an angle of attack of 20° and left sideslip angle of 16° were encountered. It might be of interest to note that the onset of the violent maneuver coincided with the attainment of the angle of attack $(\alpha \approx 8^{\circ})$ at which unpublished flight data indicates the occurrence of reduction of longitudinal stability. Also, the angle of attack of 8° corresponds to the angle of attack at which a reduction in the measured wing lift slope occurs; therefore, large wing loads were not experienced at the maximum angles of attack (fig. 5(c)). After the primary rolling motion has subsided at $t = 5$ seconds, the large lateral and longitudinal motions damp fairly well.

Another left roll time history for airplane A is presented in figure 6 for a Mach number of about 1.05. During this maneuver the favorable sideslip builds up rapidly with roll velocity and peaks at 21° at the time the airplane ceases rolling left. This large sideslip angle results in about 2g transverse acceleration. Near the time at which maximum sideslip occurs $(t \approx 4.0 \text{ sec})$ a large divergence in pitch develops in the negative direction which attains about -6.7g. The pilot applied control to stop this pitch-down and immediately reduced the control deflection, but was unable to avoid obtaining 7g when the airplane pitched up. Maximum wing loads measured during the maneuver did not approach or exceed the design limit load (fig. 6(c)); however, the fuselage load obtained from airplane weight and acceleration, and horizontal tail loads, and wing load showed maximum values of 63,000 pounds. These maximum values approximated the limit design total load of the fuselage. The measured horizontal tail loads were near limit design load (fig. 6(d)). The maximum measured vertical tail loads reached approximately 50 percent of the limit load (fig. 6(e)) at sideslip angles of 21°. It may be noted that a reduction in vertical tail load with sideslip was experienced at sideslip angles about 8°. In this maneuver, as in figure 5, when the rolling stopped, the airplane motions quickly damped.

The measured quantities for an abrupt left aileron roll for airplane B at an altitude of 30,000 feet and a Mach number of 0.70 are shown as

figure 7. Unfortunately, the roll record was lost as a result of instrument malfunctioning. As peak aileron deflection is attained, there is a steady development of left (adverse) sideslip and a progressive decrease in angle of attack. Between $t = 3$ seconds and $t = 4$ seconds, the divergence rates are accelerated considerably and negative angles of attack greater than 16° (-4.4g) and left sideslip angles as large as 26° were reached in the more violent stages of this maneuver. Maximum vertical tail loads of 5,500 pounds were measured at a sideslip angle of 26° (fig. 7(c)). It may be noted that appreciable reduction in the rate of increase of vertical tail loads with increase in sideslip angle occurred at a sideslip angle of 7°. It also should be noted that a rather large stabilizer input to oppose the motion and a small rudder input to aggravate the motion were fed in by the pilot. Recovery was affected by bringing the stabilizer and rudder controls close to their initial settings and permitting the airplane to recover. The slat motions shown result from aerodynamic and inertia loads, the slats being free floating but with the segments loosely interconnected.

The behavior of the two airplanes in the aileron rolls is similar in that large cross-coupling effects are evidenced. The airplanes are loaded primarily along the fuselage, particularly in the case of airplane A, so that considerable inertial coupling is expected (see ref. 1).

CONCLUDING REMARKS

It is evident from the time histories presented herein that violent coupled pitching and yawing motions can be encountered during abrupt aileron maneuvers. This motion is sufficiently violent to cause the pilot to lose control of the airplane and could easily result in structural failure.

High-Speed Flight Station,
National Advisory Committee for Aeronautics,
Edwards, Calif., December 27, 1954.

REFERENCE

1. Phillips, William H.: Effect of Steady Rolling on Longitudinal and Directional Stability. NACA TN 1627, 1948.

TABLE I

PHYSICAL CHARACTERISTICS OF AIRPLANE A

Wing:	
Airfoil section	Modified hexagon
Airfoil thickness ratio, percent chord	4.5
Airfoil leading and trailing edge angles, deg	8.58
Total area, sq ft	166.50
Span, ft	22.69
Mean aerodynamic chord, ft	7.84
Root chord, ft	10.58
Tip chord, ft	4.11
Taper ratio	0.39
Aspect ratio	3.09
Sweep at 0.75 chord line, deg	0.00
Incidence, deg	0.00
Dihedral, deg	0.00
Geometric twist, deg	0.00
Aileron area aft of hinge line (each), sq ft	4.04
Aileron span at hinge line (each), ft	3.25
Aileron chord aft of hinge line, percent wing chord	25.00
Aileron travel (each), deg	±12.00
Leading edge flap, type	Plain
Leading edge flap area (each), sq ft	8.38
Leading edge flap span at hinge line (each), ft	8.916
Leading edge flap chord, normal to hinge line, in.	11.50
Leading edge flap travel, deg	30.00
Trailing edge flap, type	Split
Trailing edge flap area (each), sq ft	8.61
Trailing edge flap span, ft	5.083
Trailing edge flap chord, percent wing chord	25.00
Trailing edge flap travel, deg	50.00
Horizontal tail:	
Airfoil section	Modified hexagon
Airfoil thickness ratio at root chord, percent chord	8.01
Airfoil thickness ratio outboard station 26, percent chord	4.50
Airfoil leading edge angle, deg	11.96
Airfoil trailing edge angle, deg	8.77
Total area, sq ft	43.24
Span, ft	13.77
Mean aerodynamic chord, ft	3.34
Root chord, ft	4.475
Tip chord, ft	1.814
Taper ratio	0.405
Aspect ratio	4.38
Sweep at leading edge, deg	21.14
Sweep at trailing edge, deg	0
Dihedral, deg	0
Travel, leading edge up, deg	6
Travel, leading edge down, deg	17
Hinge line location, percent root chord	46.46

TABLE I.- Concluded

PHYSICAL CHARACTERISTICS OF AIRPLANE A

Vertical tail:	
Airfoil section	Modified hexagon
Airfoil thickness ratio, percent chord	4.5
Airfoil leading and trailing edge angles, deg	8.58
Area, sq ft	23.73
Span, ft	5.59
Mean aerodynamic chord, ft	4.69
Root chord, ft	6.508
Tip chord, ft	1.93
Taper ratio	0.292
Aspect ratio	1.315
Sweep at leading edge, deg	45.00
Sweep at trailing edge, deg	9.39
Rudder area, aft of hinge line, sq ft	5.441
Rudder span at hinge line, ft	3.535
Rudder root chord, ft	1.98
Rudder tip chord, ft	1.097
Rudder travel, deg	±20
Fuselage:	
Length including boom, ft	66.75
Maximum width, ft	6.08
Maximum height, ft	4.81
Base area, sq ft	7.94
Power Plant:	
Two Westinghouse J-34-WE-17 with afterburner	
Thrust each engine (guarantee SL) lbs - afterburner	4,850
Military	3,370
Airplane Weight, lb:	
Basic (without fuel, oil, water, pilot)	16,120
Total (full fuel, oil, water - no pilot)	21,900
Center of gravity location, percent $\bar{c}$:	
Basic weight - gear down	2.63
Total weight - gear down	4.59
Total weight - gear up	3.91
Moments of inertia (estimated for total weight):	
I_X, slug-ft^2	4,100
I_Y, slug-ft^2	61,200
I_Z, slug-ft^2	65,100
I_{XZ}, slug-ft^2	4,200
Inclination of principal axis (estimated) below reference axis at nose, deg	3

TABLE II

PHYSICAL CHARACTERISTICS OF AIRPLANE B

Wing:	
Airfoil section	NACA 64A007
Total area (including aileron and 83.84 sq ft covered by fuselage), sq ft	376.02
Span, ft	36.58
Mean aerodynamic chord, ft	11.33
Root chord, ft	15.86
Tip chord, ft	4.76
Taper ratio	.30
Aspect ratio	3.56
Sweep at 0.25 chord line, deg	.45
Incidence, deg	0
Dihedral, deg	0
Geometric twist, deg	0
Aileron area aft of hinge line (each), sq ft	19.32
Aileron span at hinge line (each), ft	7.81
Aileron chord aft of hinge line, percent wing chord	25.00
Aileron travel (each), deg	±15.00
Irreversible hydraulic boost and artificial feel	
Aerodynamic balance	None
Static balance	Internal lead weights
Leading edge slat span, equivalent, ft	12.71
Leading edge slat segments	5
Leading edge slat spanwise location, inboard end, percent wing semispan	24.6
Leading edge slat spanwise location, outboard end, percent wing semispan	94.1
Leading edge slat ratio of slat chord to wing chord (parallel to fuselage reference line), percent	20.0
Leading edge slat rotation, maximum, deg	15.0
Horizontal tail:	
Airfoil section	NACA 65A003.5
Total area (including 31.65 sq ft covered by fuselage), sq ft	98.86
Span, ft	18.72
Mean aerodynamic chord, ft	5.83
Root chord, ft	8.14
Tip chord, ft	2.46
Taper ratio	0.30
Aspect ratio	3.54
Sweep at 0.25 chord line, deg	45
Dihedral, deg	0
Travel, leading edge up, deg	5
Travel, leading edge down, deg	25
Irreversible hydraulic boost and artificial feel	
Vertical tail:	
Airfoil section	NACA 65A003.5
Area (excluding 3.16 sq ft dorsal fin and 2.11 sq ft blanketed by fuselage), sq ft	33.54
Span (unblanketed), ft	6.14
Mean aerodynamic chord, ft	5.83

TABLE II.- Concluded

PHYSICAL CHARACTERISTICS OF AIRPLANE B

Root chord, ft	7.75
Tip chord, ft	3.32
Taper ratio	0.428
Aspect ratio	1.06
Sweep at 0.25 chord line, deg	45
Rudder area, aft of hinge line, sq ft	6.3
Rudder span at hinge line, ft	3.33
Rudder root chord, ft	2.27
Rudder tip chord, ft	1.50
Rudder travel, deg	±20
Rudder spanwise location, inboard end, percent rudder span	3.6
Rudder spanwise location, outboard end, percent rudder span	57.9
Rudder chord, percent vertical tail chord	30.00
Rudder aerodynamic balance	Overhanging, unsealed
Fuselage:	
Length (afterburner nozzle closed), ft	45.64
Maximum width, ft	5.58
Maximum depth over canopy, ft	6.37
Side area (total), sq ft	230.92
Fineness ratio (afterburner nozzle closed)	7.86
Clean airplane:	
Total surface area, sq ft	1546.58
Total frontal area, sq ft	53.82
Speed brake:	
Surface area, sq ft	14.14
Maximum deflection, deg	50
Power plant:	
One Pratt and Whitney J57-P7 turbojet engine with afterburner	
Thrust (guarantee sea level), afterburner, lb	15,000
Military, lb	9,220
Normal, lb	8,000
Airplane weight, lb:	
Basic (without fuel, oil, water, pilot)	19,662
Total (full fuel, oil, water, pilot)	24,800
Center-of-gravity location, percent $\bar{c}$:	
Total weight - gear down	31.80
Total weight - gear up	31.80
Moments of inertia (estimated for total weight):	
I_X, slug-ft^2	11,103
I_Y, slug-ft^2	59,248
I_Z, slug-ft^2	67,279
I_{XZ}, slug-ft^2	941
Inclination of principal axis (estimated) below reference axis at nose, deg	0.8

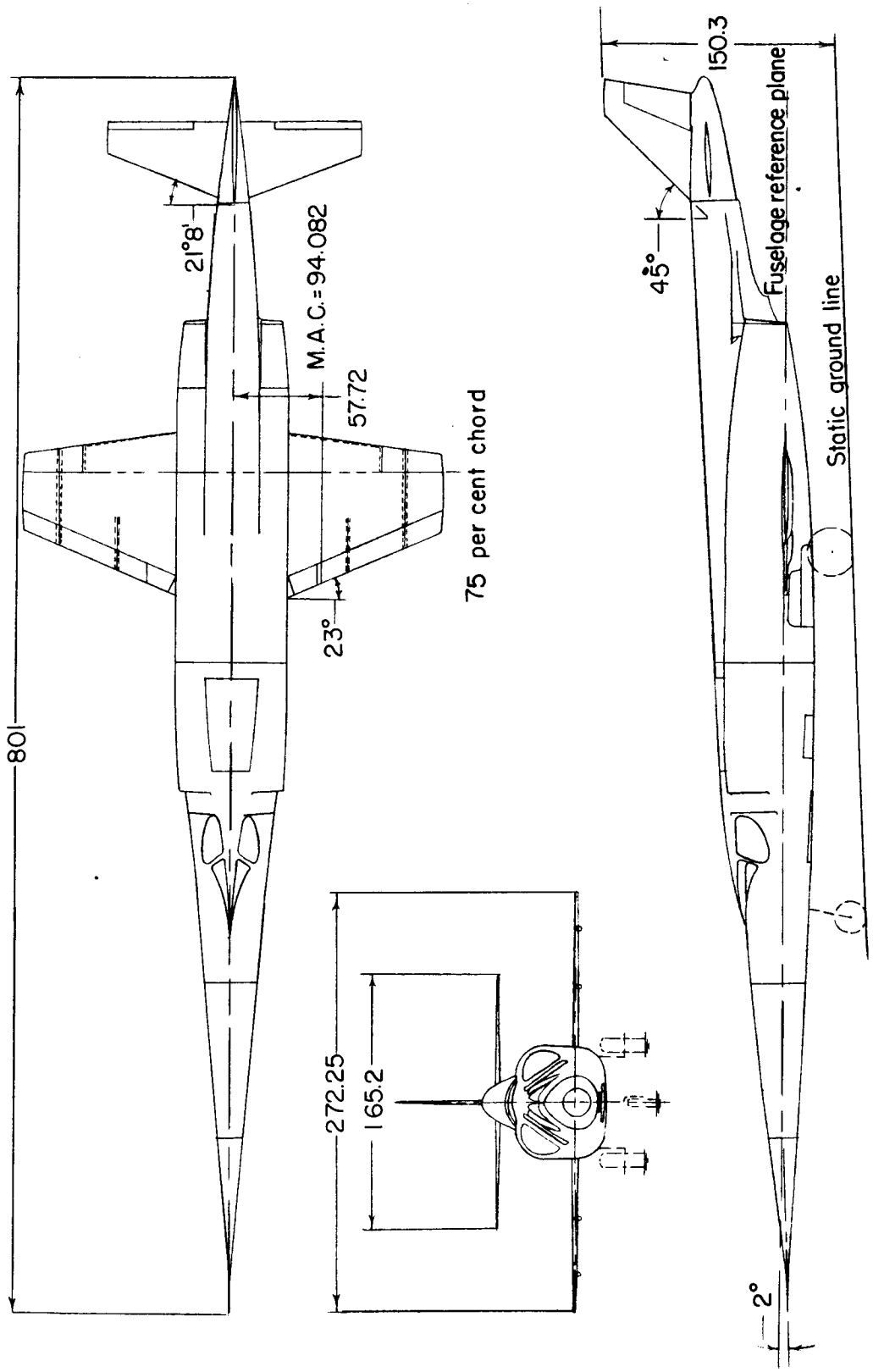

Figure 1.- A three-view drawing of airplane A. All dimensions in inches.

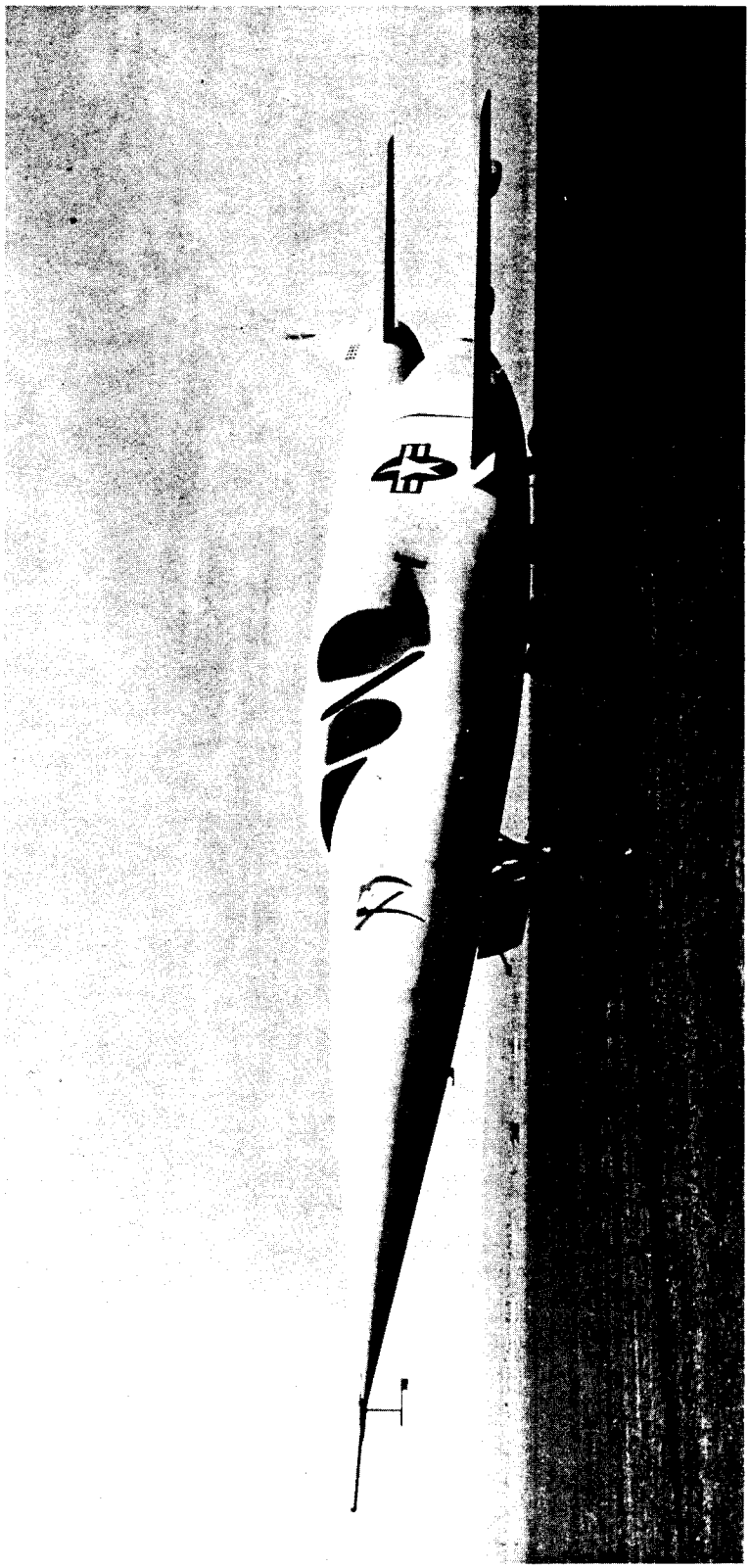

L-87520

(a) Three-quarter front view.

Figure 2.- Photographs of airplane A.

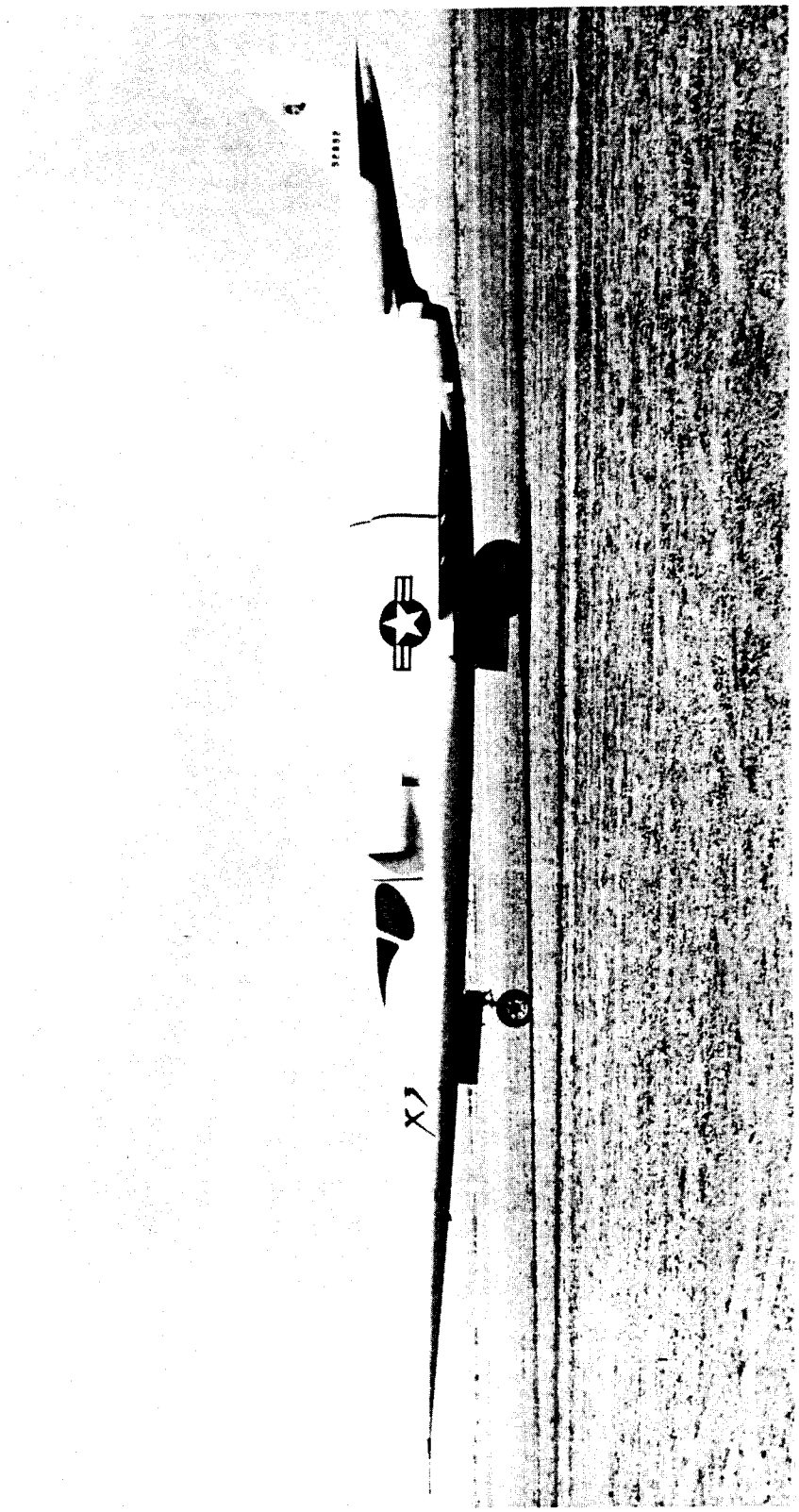

L-87521

(b) Side view.

Figure 2.- Concluded.

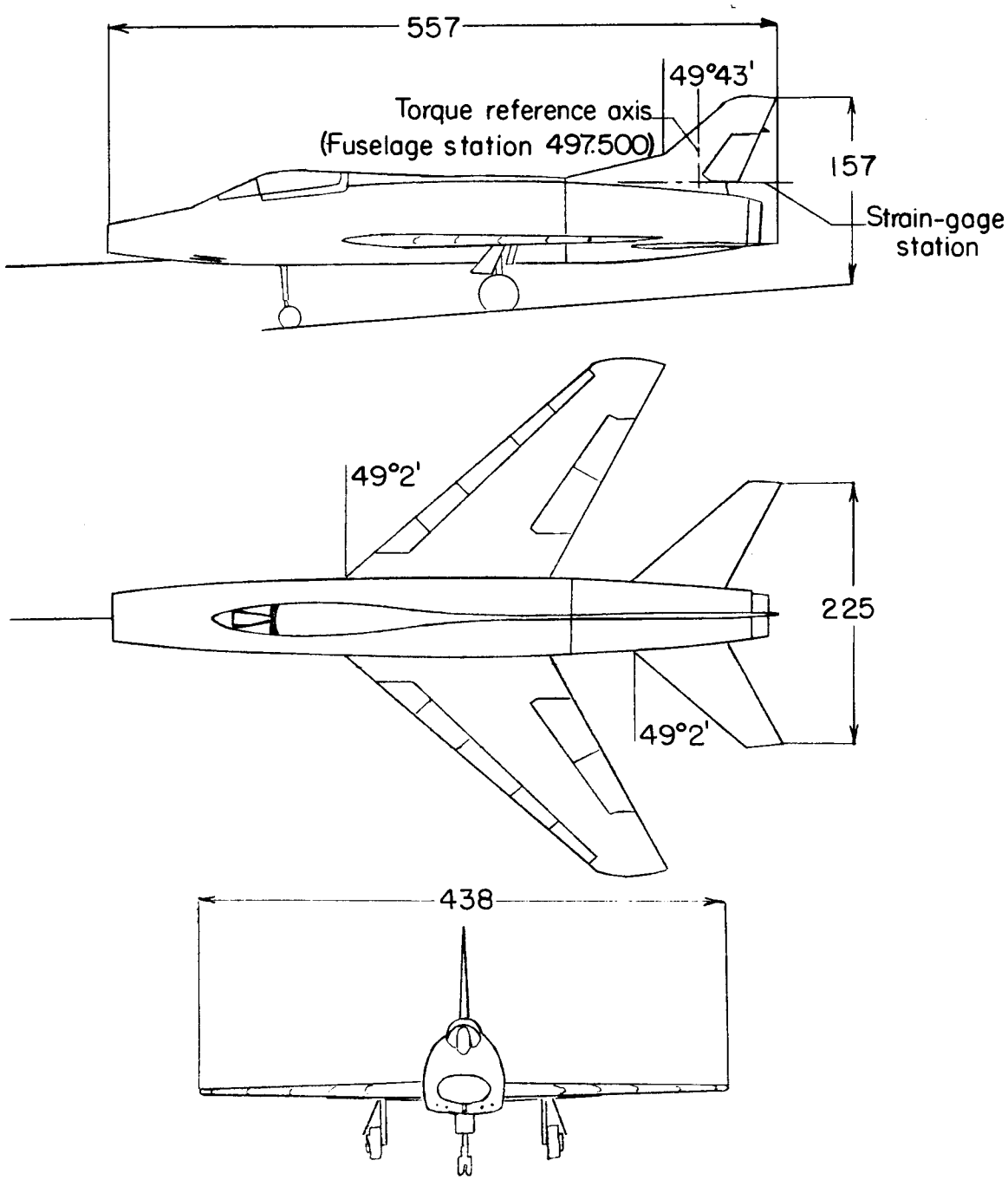

Figure 3.- Three-view drawing of airplane B. All dimensions in inches.

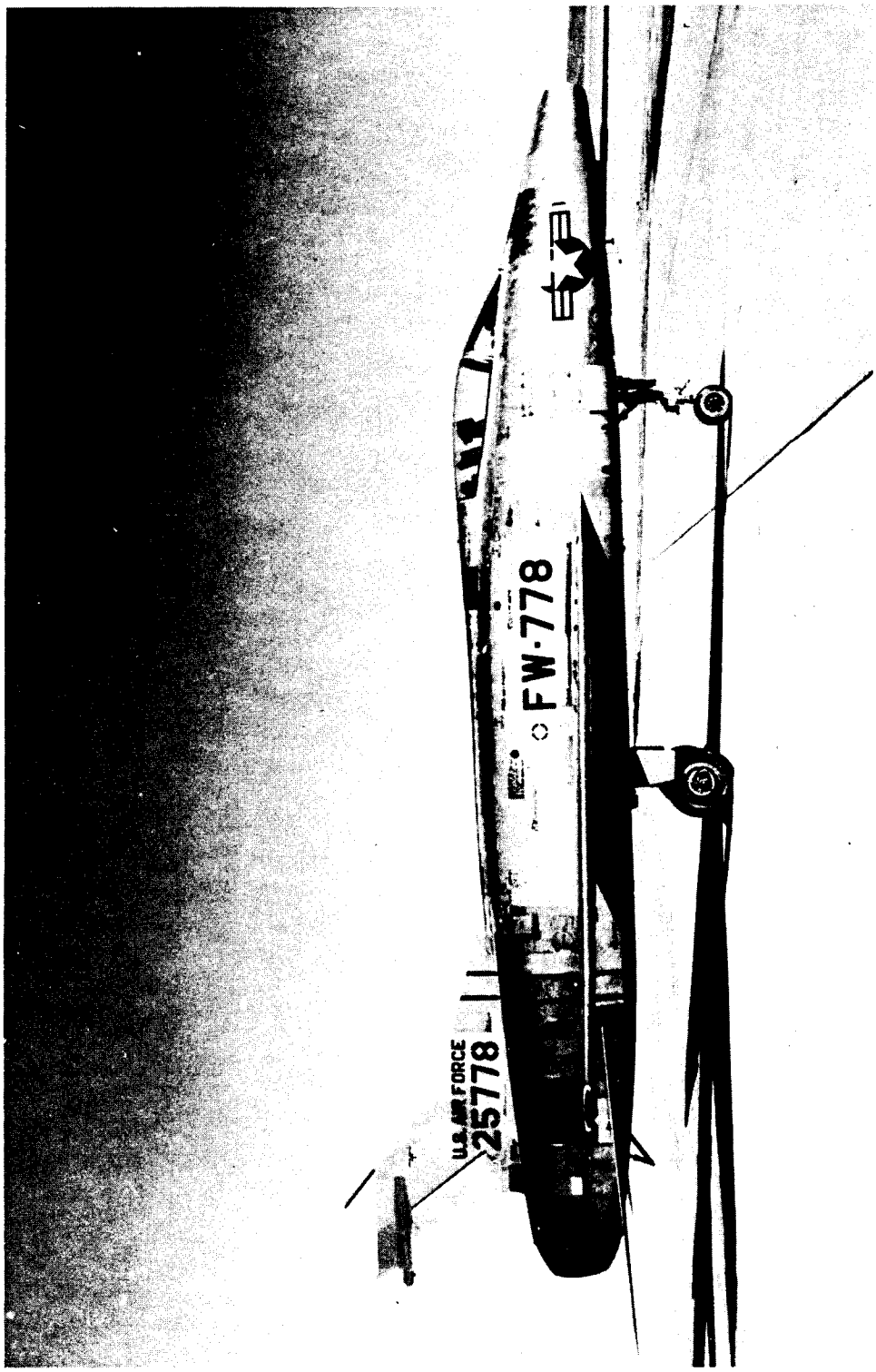

L-87522

(a) Side view.

Figure 4.- Photographs of airplane B.

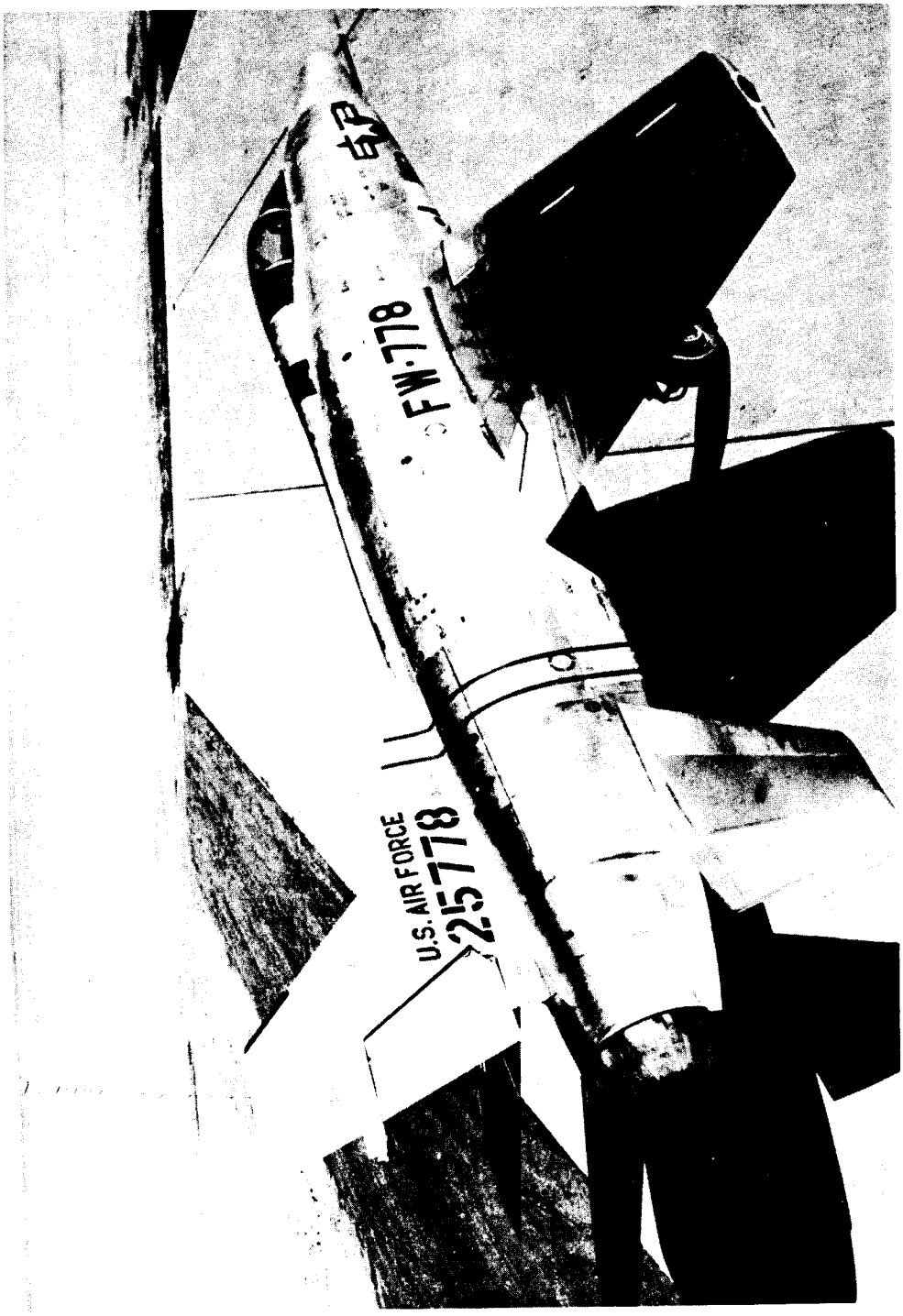

L-87523

(b) Three-quarter rear view.

Figure 4.- Continued.

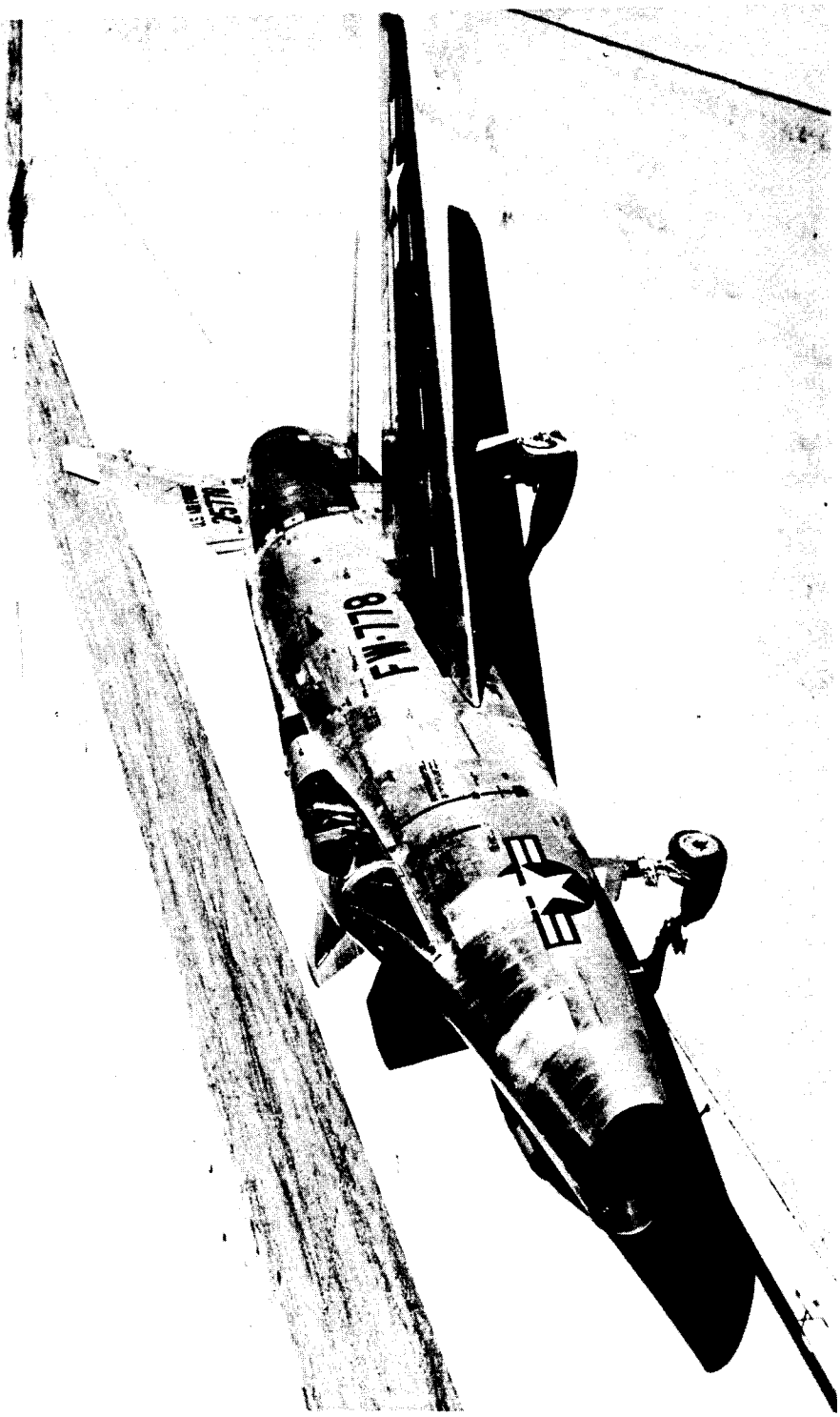

L-87524

(c) Three-quarter front view.

Figure 4.- Concluded.

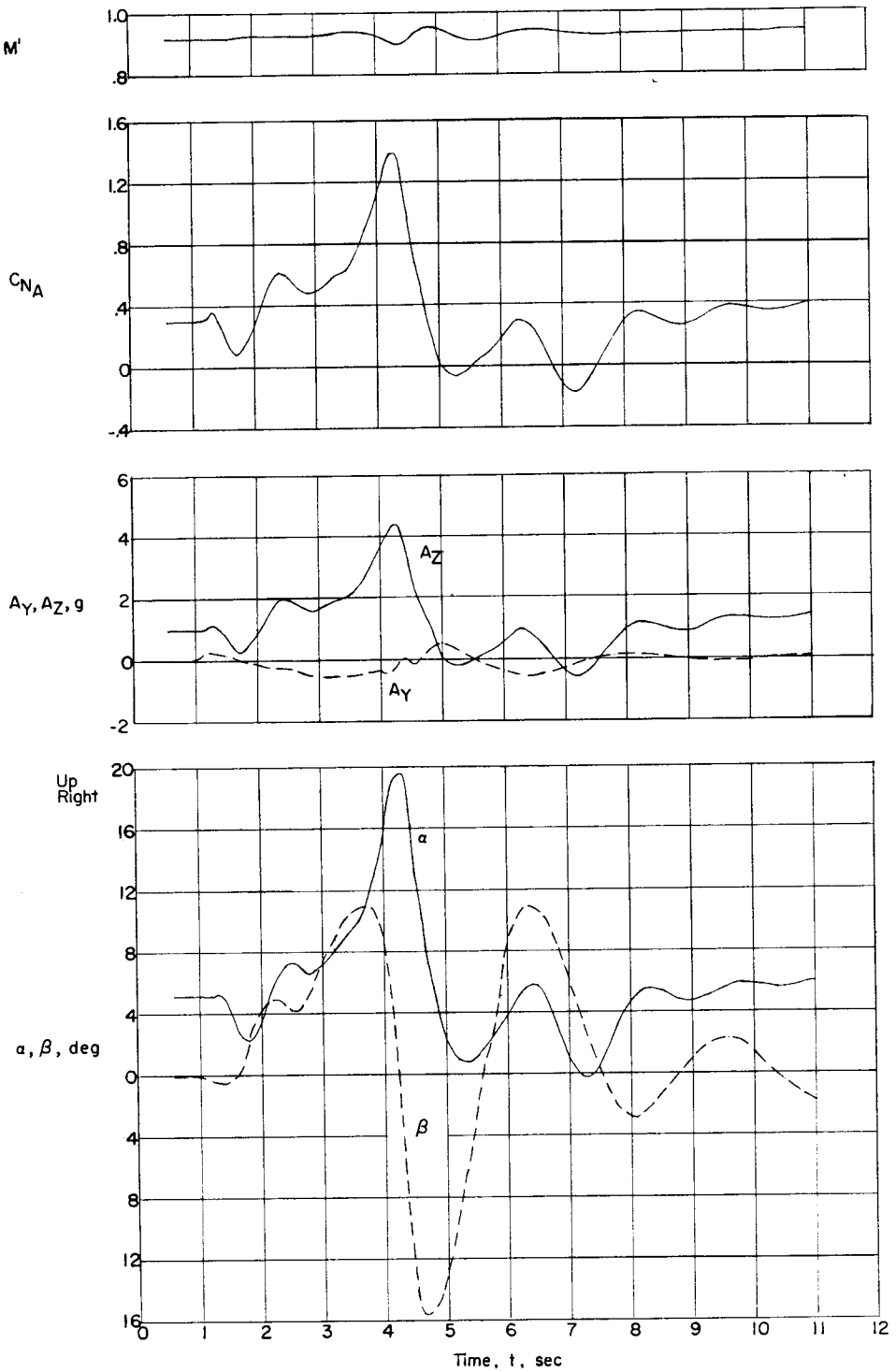

(a) Stability and control plots.

Figure 5.- Time history of quantities measured during an abrupt aileron roll with airplane A at $M \approx 0.92$. $h_p \approx 30{,}000$ feet.

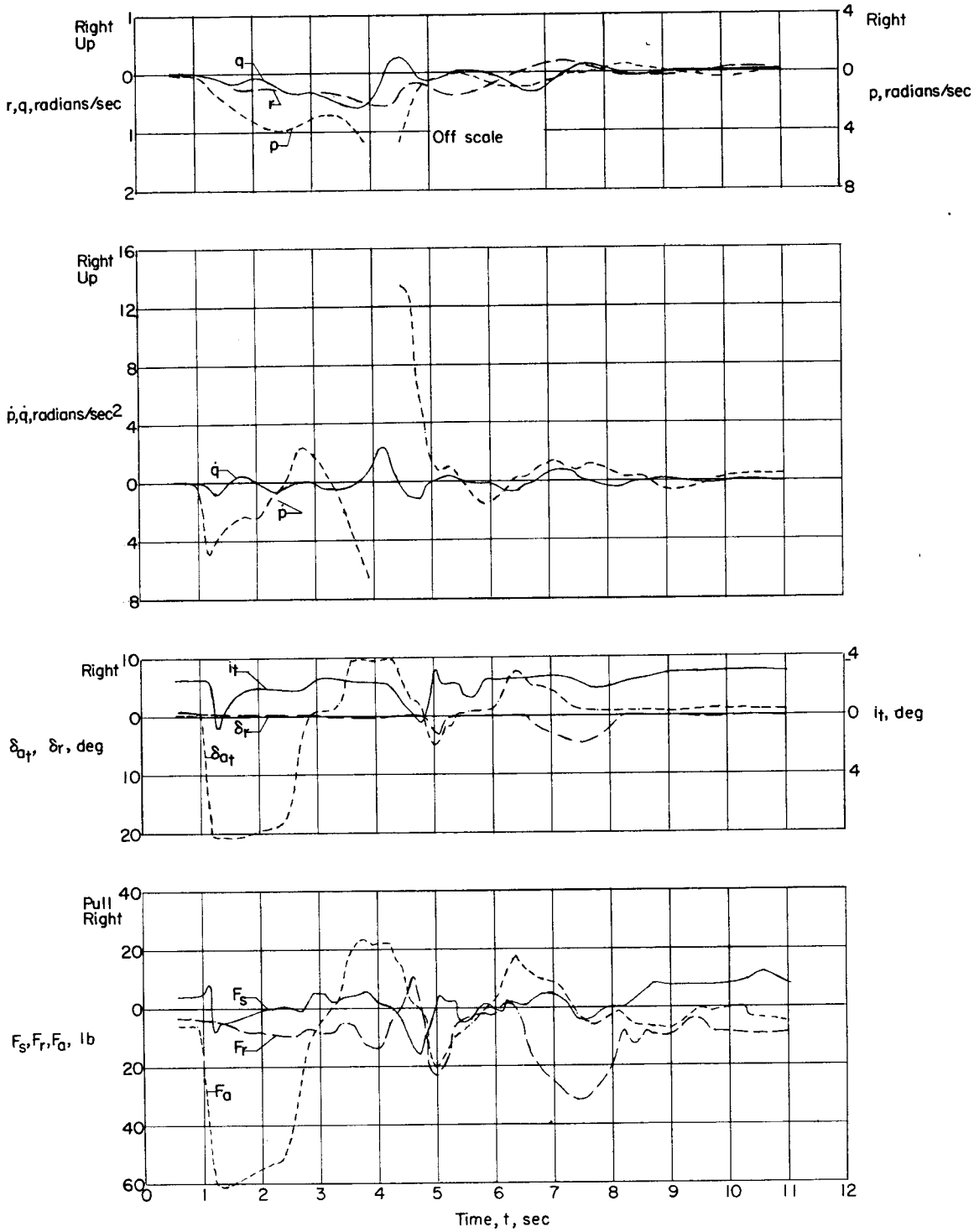

(b) Stability and control plots.

Figure 5.- Continued.

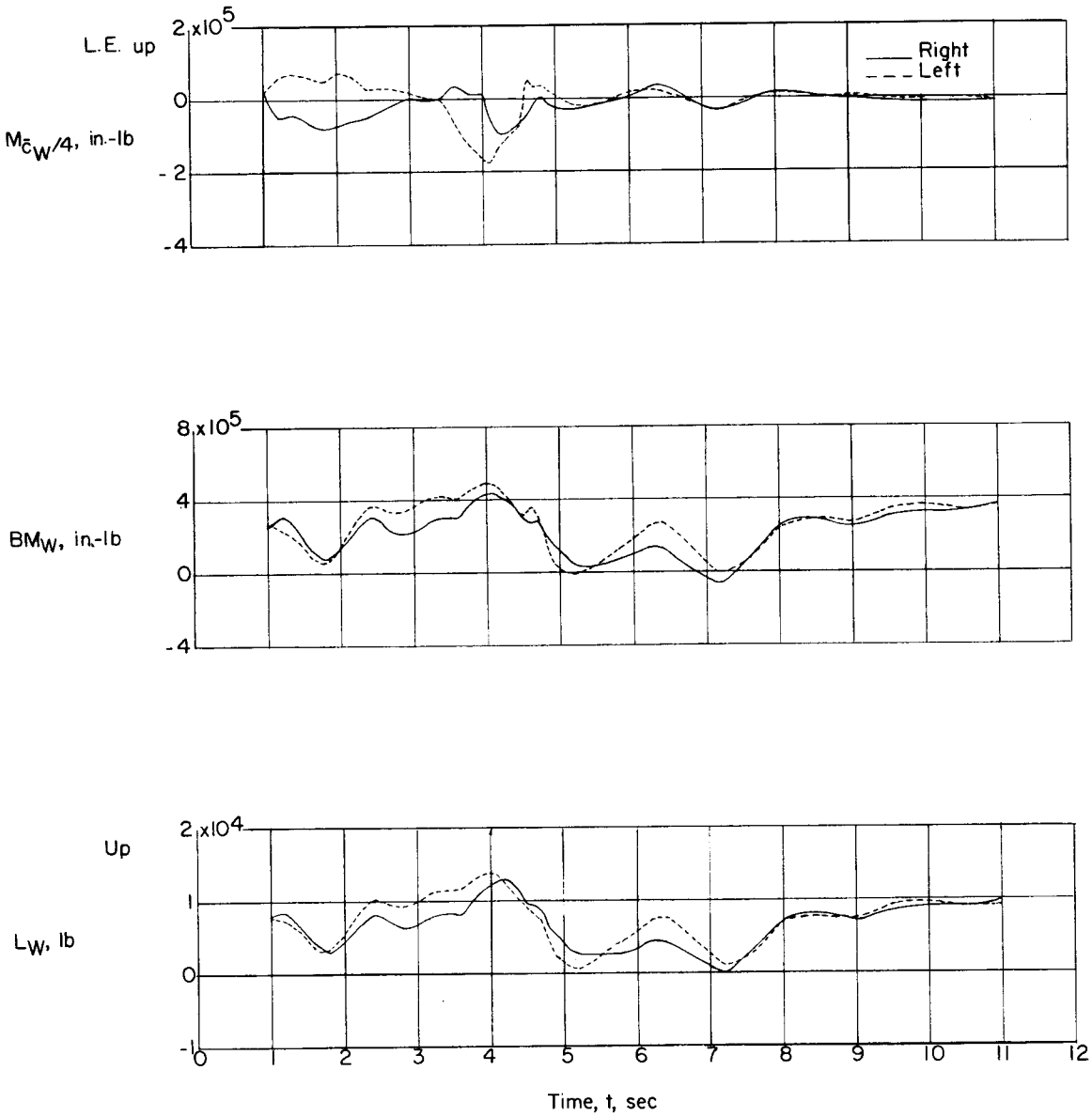

(c) Wing structural loads.

Figure 5.- Continued.

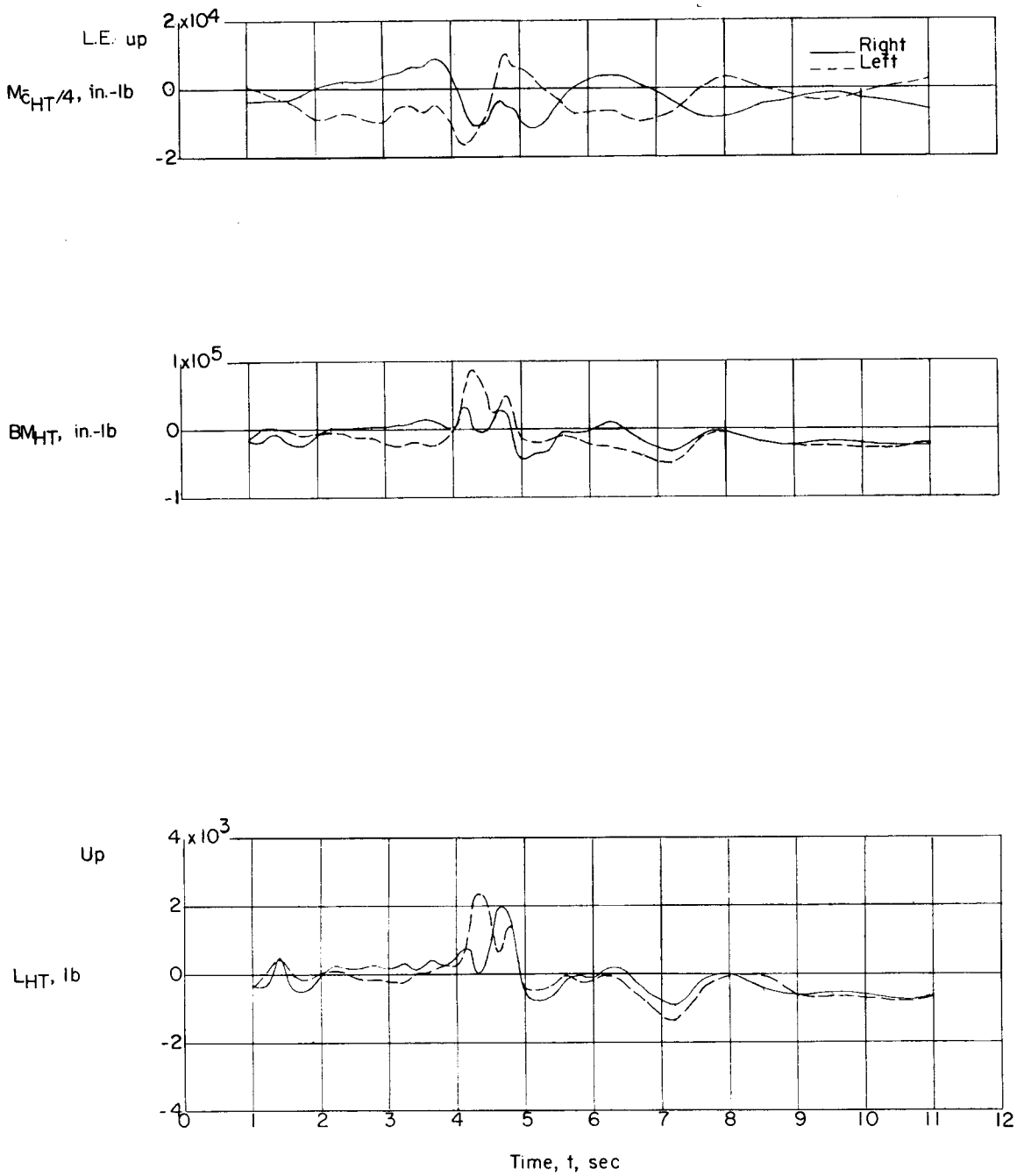

(d) Horizontal tail structural loads.

Figure 5.- Continued.

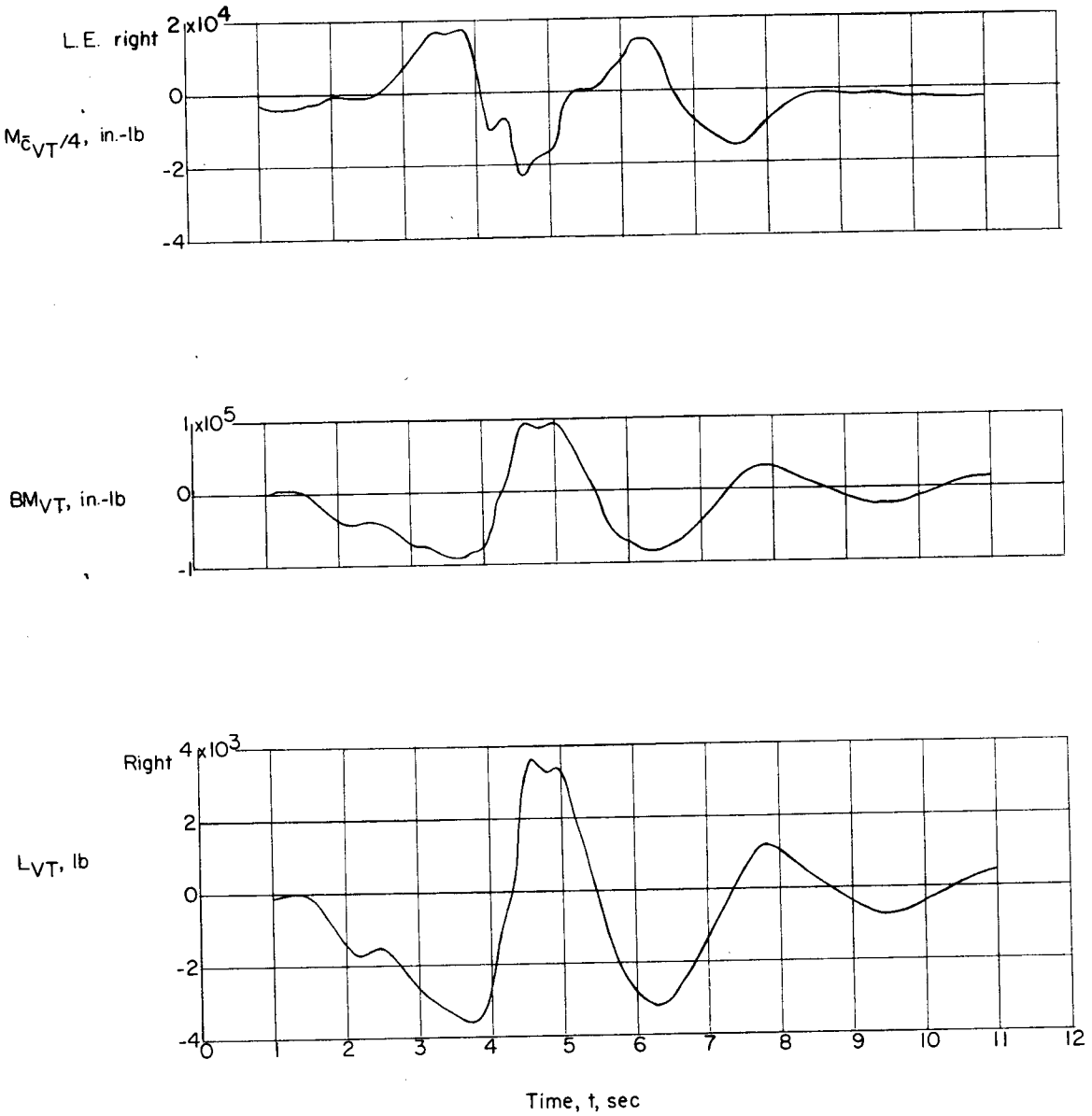

(e) Vertical tail structural loads.

Figure 5.- Concluded.

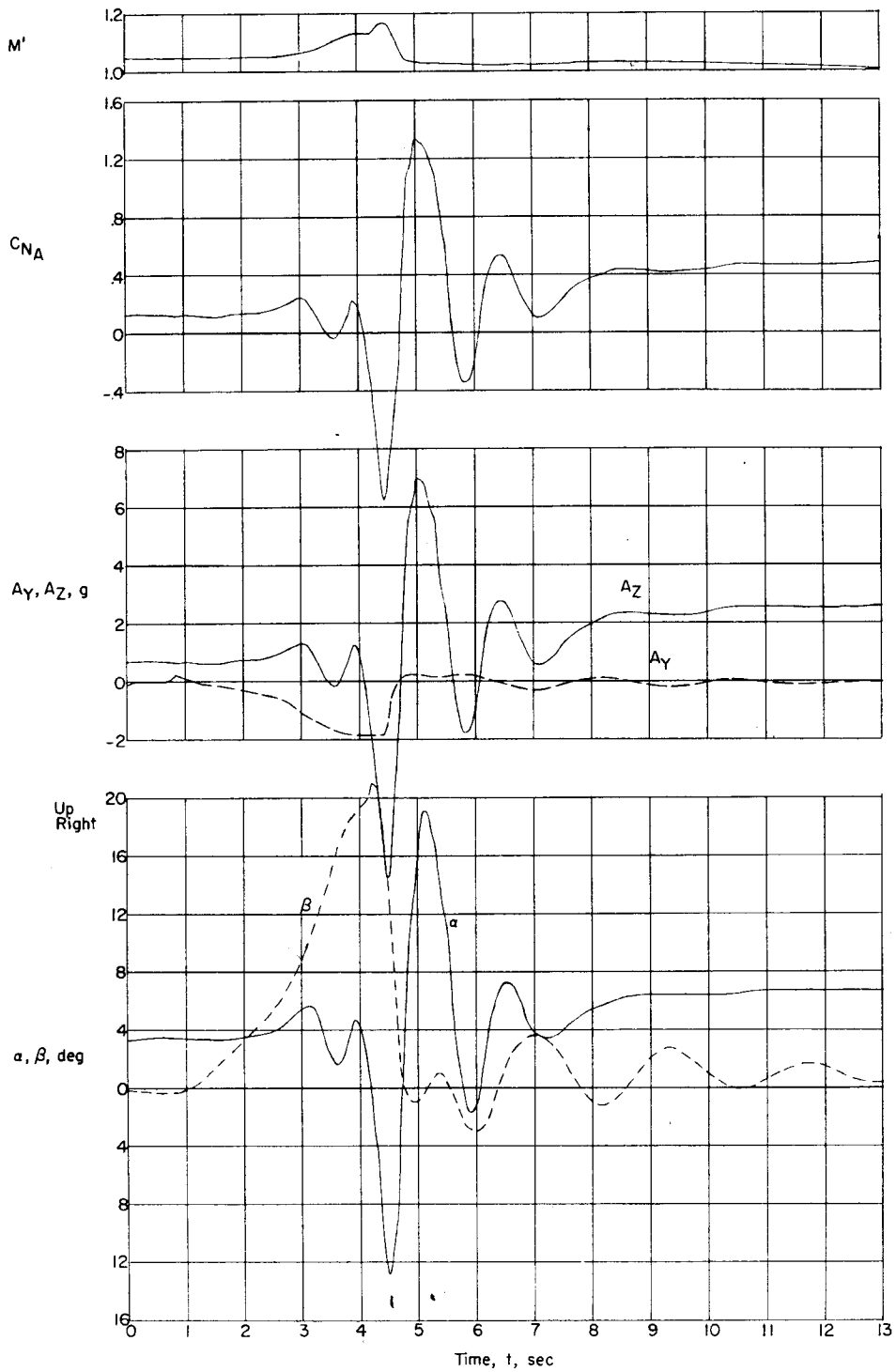

(a) Stability and control plots.

Figure 6.- Time history of quantities measured during an abrupt aileron roll with airplane A at $M = 1.05$. $h_p \approx 30{,}000$ feet.

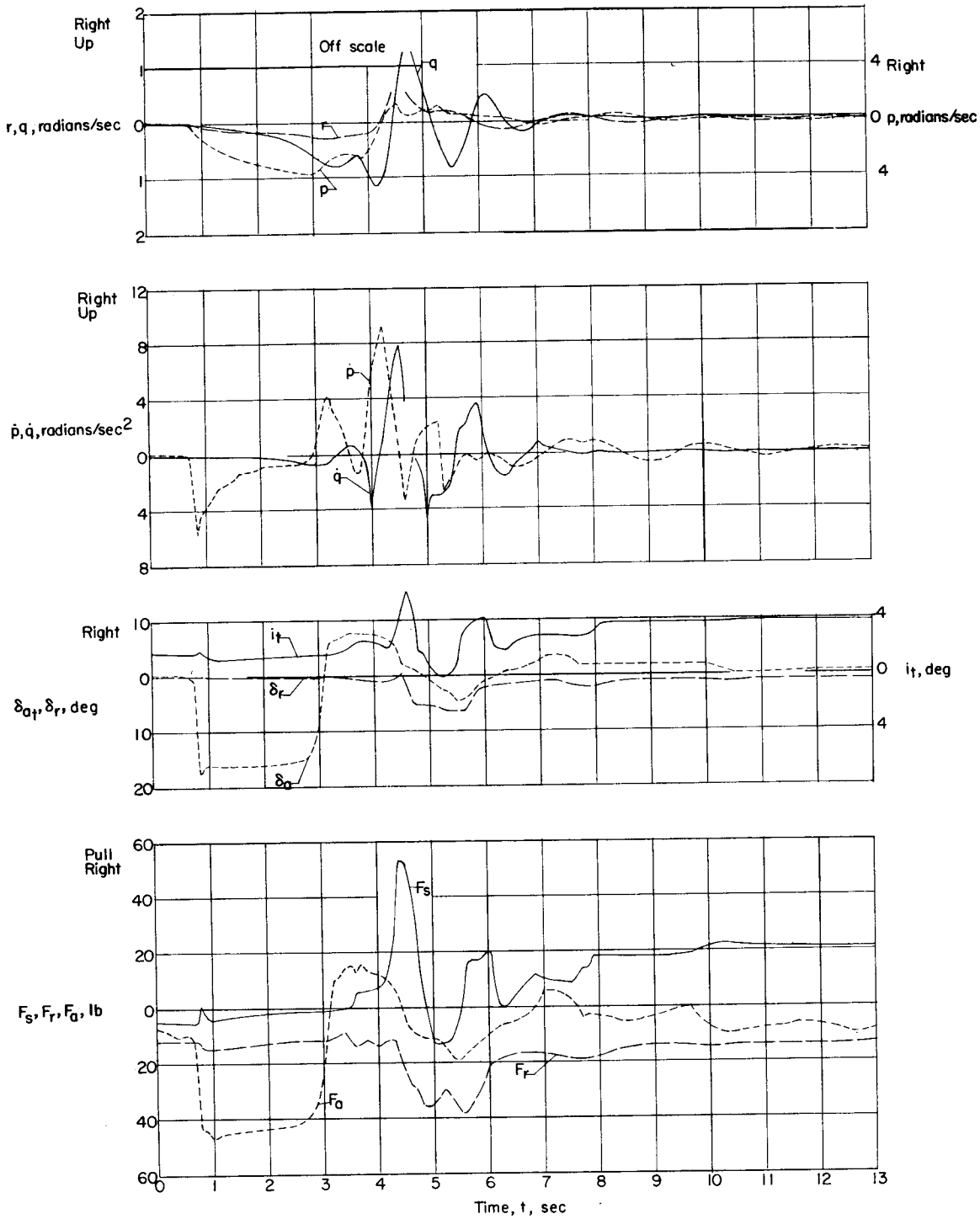

(b) Stability and control plots.

Figure 6.- Continued.

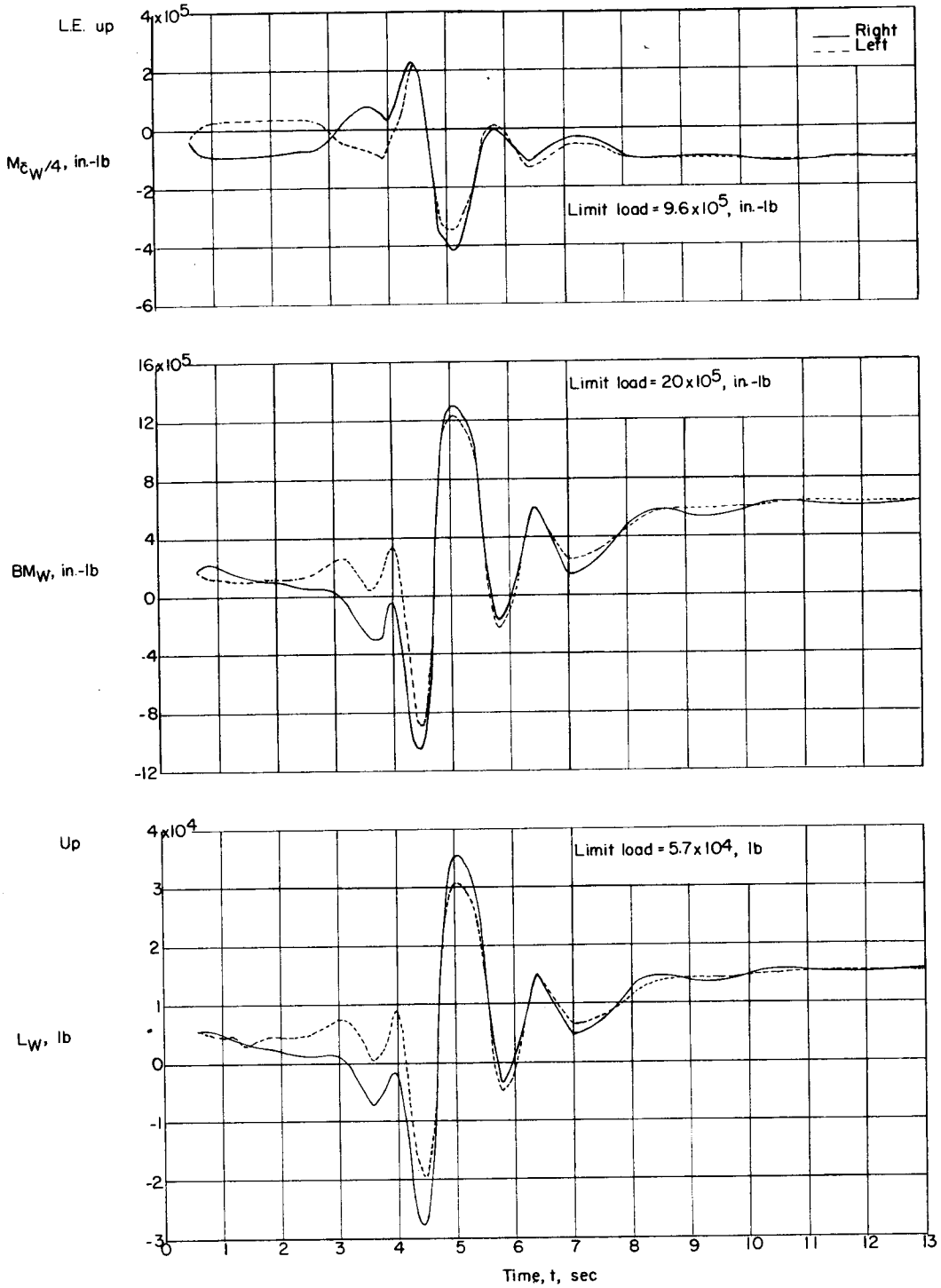

(c) Wing structural loads.

Figure 6.- Continued.

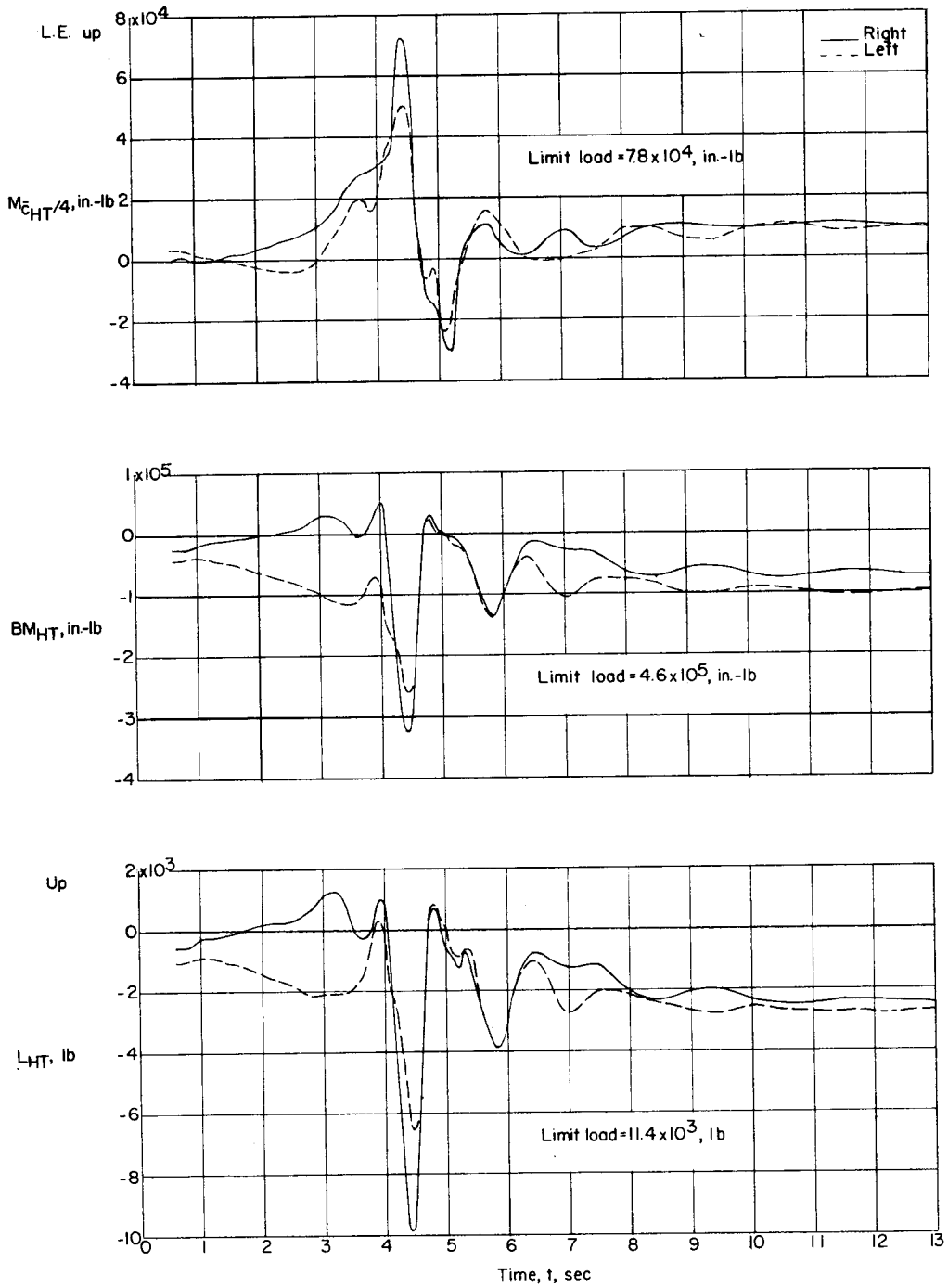

(d) Horizontal tail structural loads.

Figure 6.- Continued.

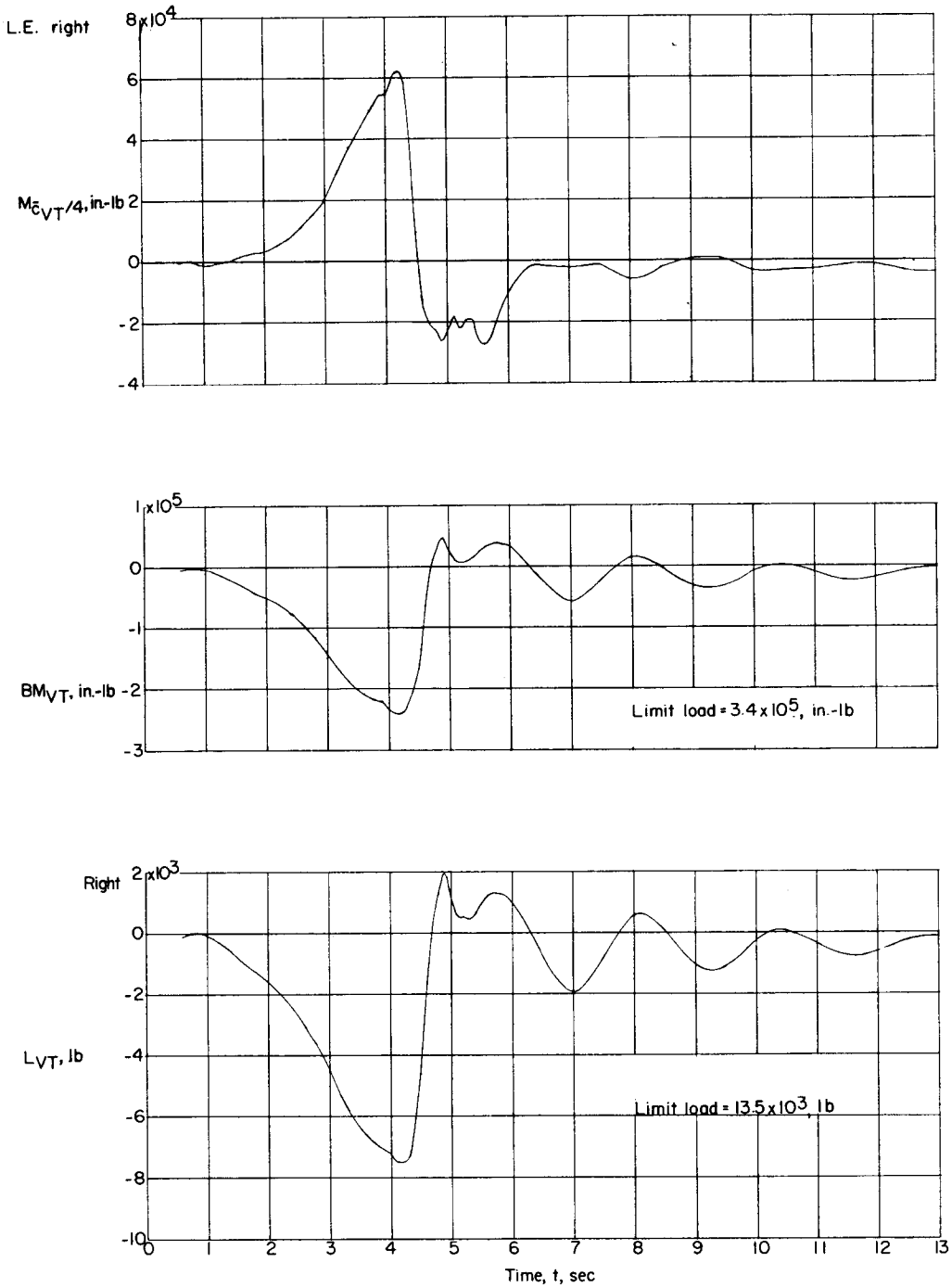

(e) Vertical tail structural loads.

Figure 6.- Concluded.

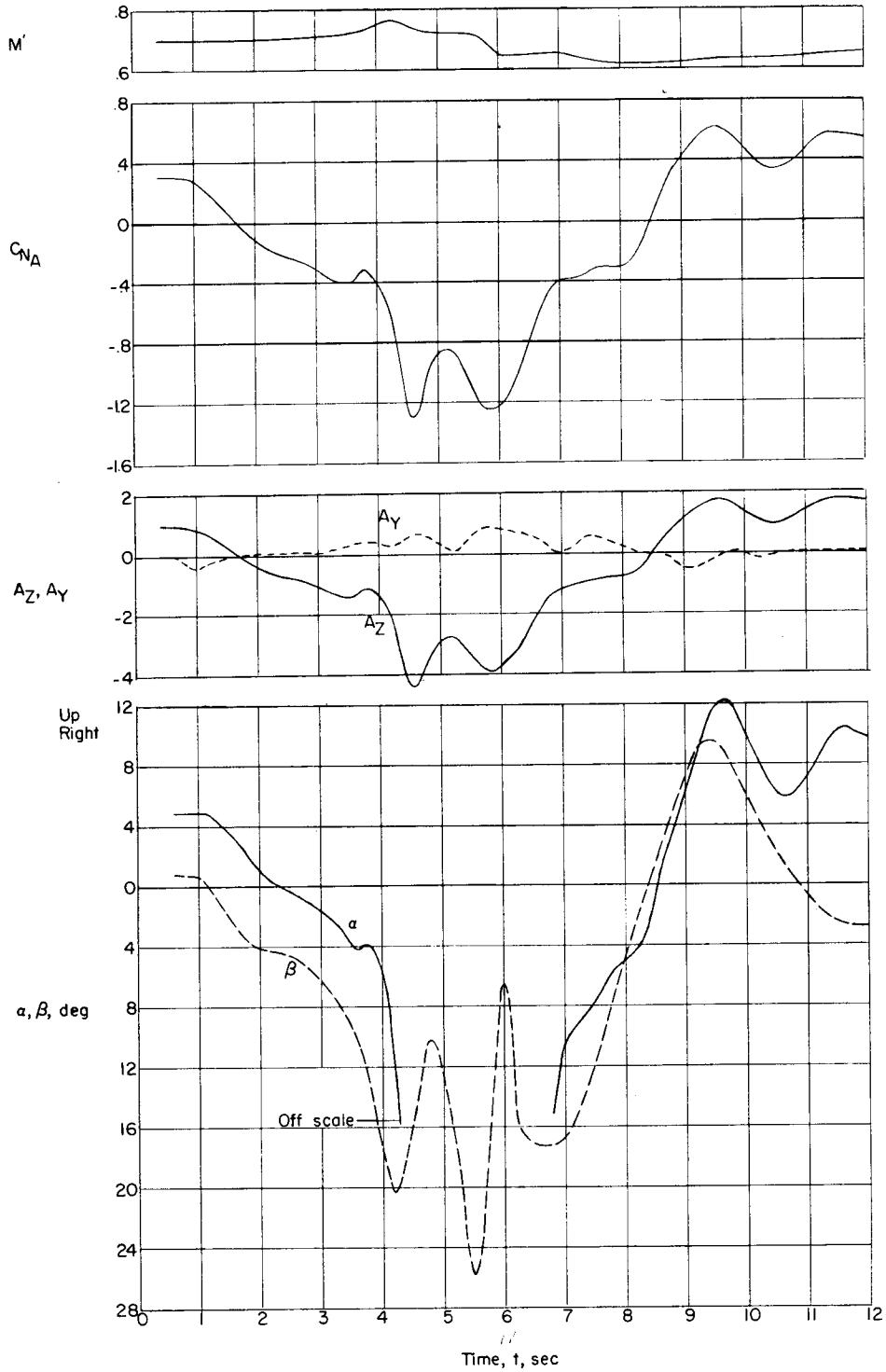

(a) Stability and control plots.

Figure 7.- Time history of quantities measured during abrupt aileron roll with airplane B at $M = 0.70$. $h_p \approx 30{,}000$ feet.

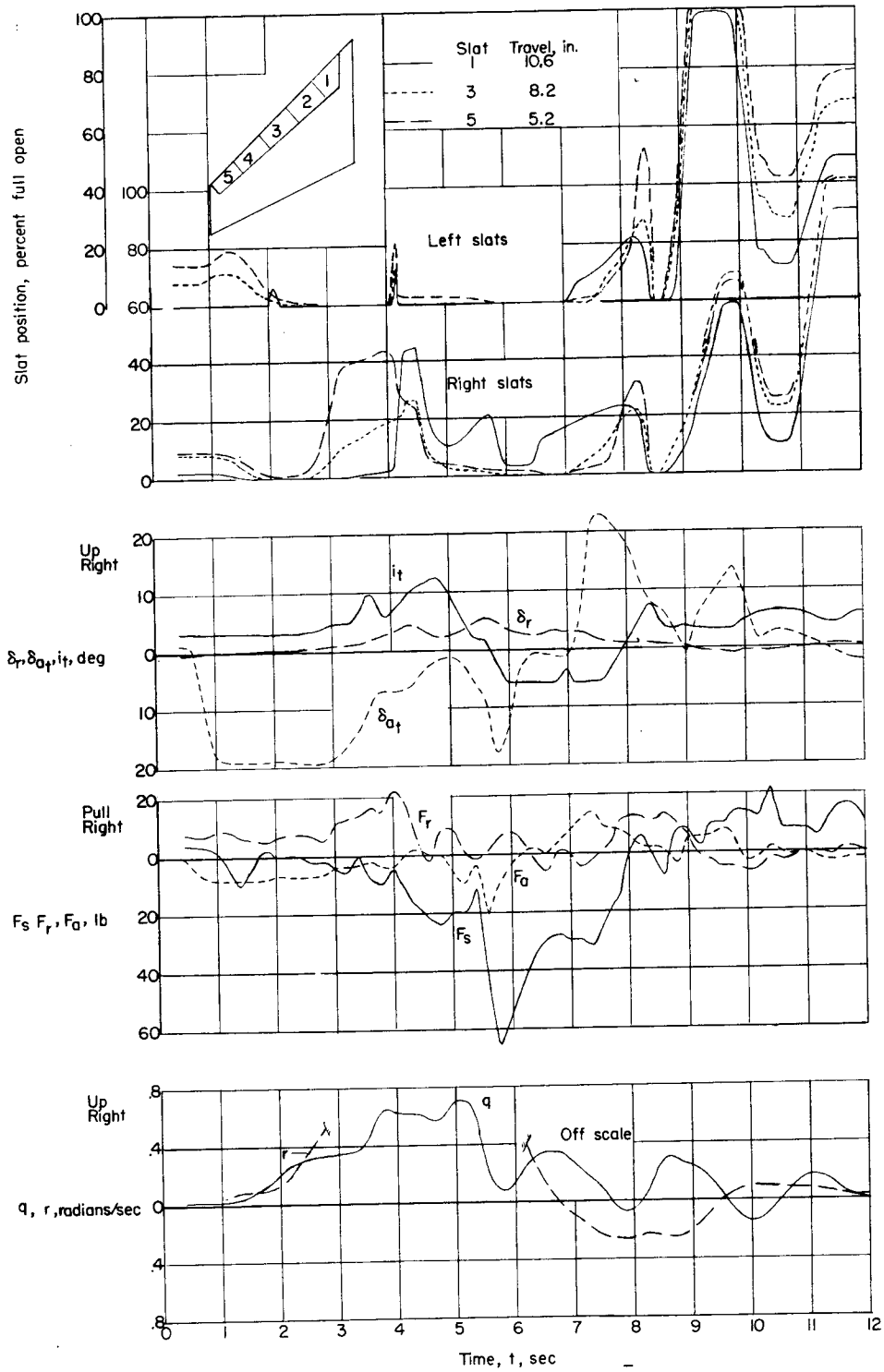

(b) Stability and control plots.

Figure 7.- Continued.

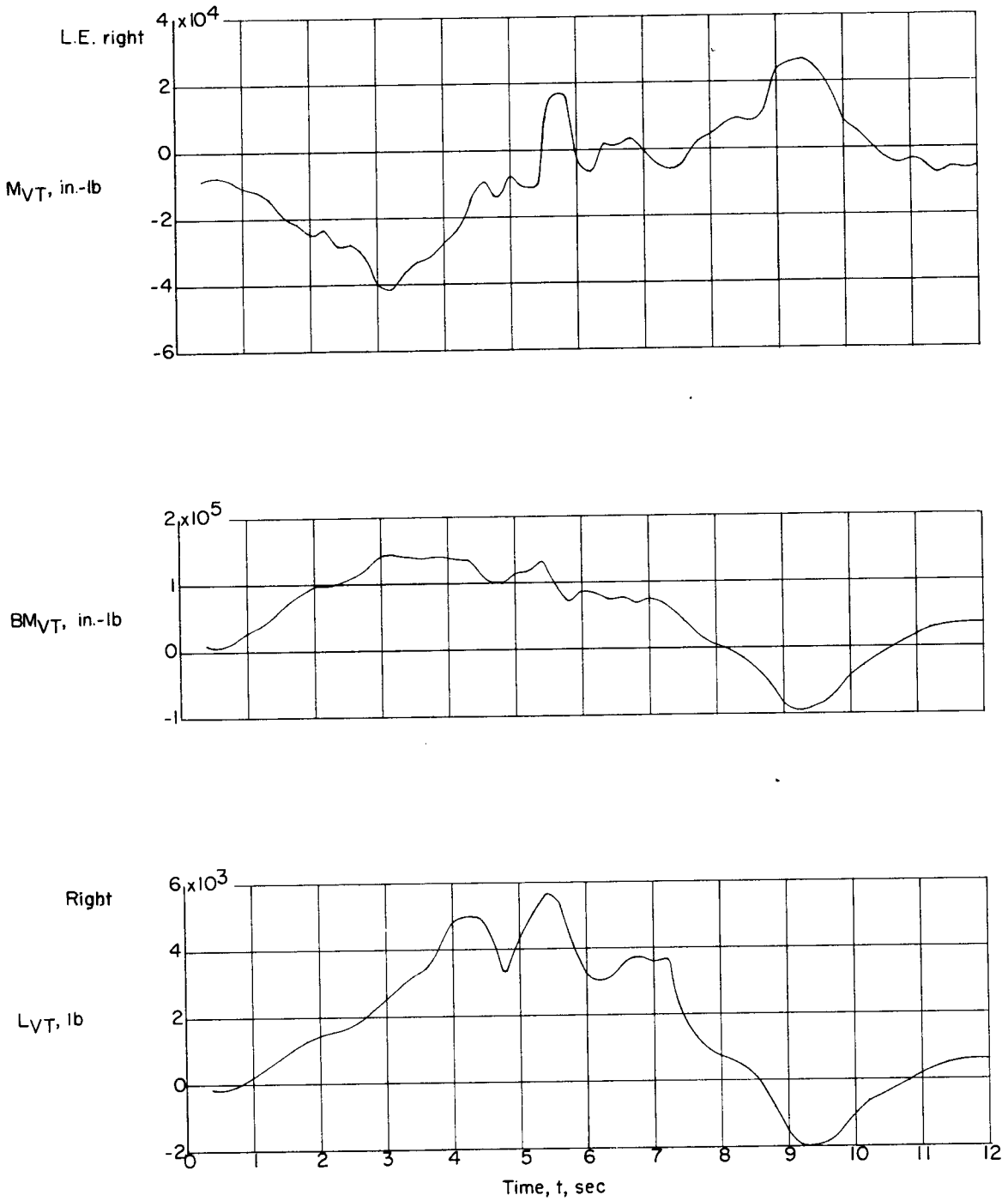

(c) Vertical tail structural loads.

Figure 7.- Concluded.

NACA RM H55A13
National Advisory Committee for Aeronautics.
FLIGHT EXPERIENCE WITH TWO HIGH-SPEED AIRPLANES HAVING VIOLENT LATERAL-LONGITUDINAL COUPLING IN AILERON ROLLS. NACA High-Speed Flight Station. February 1955. 30p. diagrs., photos., 2 tabs. (NACA RM H55A13)
[redacted]

During flight tests of two high-speed airplane configurations violent cross-coupled lateral and longitudinal motions were encountered following abrupt rudder-fixed aileron rolls at Mach numbers between 0.7 and 1.05.

Copies obtainable from NACA, Washington

[redacted]

1. Stability, Longitudinal - Static (1.8.1.1.1)
2. Stability, Lateral - Static (1.8.1.1.2)
3. Stability, Longitudinal - Dynamic (1.8.1.2.1)
4. Stability, Lateral and Directional - Dynamic (1.8.1.2.2)
5. Flying Qualities (1.8.5)
6. Mass and Gyroscopic Problems (1.8.6)
7. Loads, Maneuvering - Wings (4.1.1.1.2)
8. Loads, Maneuvering - Tail (4.1.1.2.2)

(over)

[redacted]

NACA RM H55A13
National Advisory Committee for Aeronautics.
FLIGHT EXPERIENCE WITH TWO HIGH-SPEED AIRPLANES HAVING VIOLENT LATERAL-LONGITUDINAL COUPLING IN AILERON ROLLS. NACA High-Speed Flight Station. February 1955. 30p. diagrs., photos., 2 tabs. (NACA RM H55A13)
[redacted]

During flight tests of two high-speed airplane configurations violent cross-coupled lateral and longitudinal motions were encountered following abrupt rudder-fixed aileron rolls at Mach numbers between 0.7 and 1.05.

Copies obtainable from NACA, Washington

[redacted]

1. Stability, Longitudinal - Static (1.8.1.1.1)
2. Stability, Lateral - Static (1.8.1.1.2)
3. Stability, Longitudinal - Dynamic (1.8.1.2.1)
4. Stability, Lateral and Directional - Dynamic (1.8.1.2.2)
5. Flying Qualities (1.8.5)
6. Mass and Gyroscopic Problems (1.8.6)
7. Loads, Maneuvering - Wings (4.1.1.1.2)
8. Loads, Maneuvering - Tail (4.1.1.2.2)

(over)

[redacted]

NACA RM H55A13
National Advisory Committee for Aeronautics.
FLIGHT EXPERIENCE WITH TWO HIGH-SPEED AIRPLANES HAVING VIOLENT LATERAL-LONGITUDINAL COUPLING IN AILERON ROLLS. NACA High-Speed Flight Station. February 1955. 30p. diagrs., photos., 2 tabs. (NACA RM H55A13)
[redacted]

During flight tests of two high-speed airplane configurations violent cross-coupled lateral and longitudinal motions were encountered following abrupt rudder-fixed aileron rolls at Mach numbers between 0.7 and 1.05.

Copies obtainable from NACA, Washington

[redacted]

1. Stability, Longitudinal - Static (1.8.1.1.1)
2. Stability, Lateral - Static (1.8.1.1.2)
3. Stability, Longitudinal - Dynamic (1.8.1.2.1)
4. Stability, Lateral and Directional - Dynamic (1.8.1.2.2)
5. Flying Qualities (1.8.5)
6. Mass and Gyroscopic Problems (1.8.6)
7. Loads, Maneuvering - Wings (4.1.1.1.2)
8. Loads, Maneuvering - Tail (4.1.1.2.2)

(over)

[redacted]

NACA RM H55A13
National Advisory Committee for Aeronautics.
FLIGHT EXPERIENCE WITH TWO HIGH-SPEED AIRPLANES HAVING VIOLENT LATERAL-LONGITUDINAL COUPLING IN AILERON ROLLS. NACA High-Speed Flight Station. February 1955. 30p. diagrs., photos., 2 tabs. (NACA RM H55A13)
[redacted]

During flight tests of two high-speed airplane configurations violent cross-coupled lateral and longitudinal motions were encountered following abrupt rudder-fixed aileron rolls at Mach numbers between 0.7 and 1.05.

Copies obtainable from NACA, Washington

[redacted]

1. Stability, Longitudinal - Static (1.8.1.1.1)
2. Stability, Lateral - Static (1.8.1.1.2)
3. Stability, Longitudinal - Dynamic (1.8.1.2.1)
4. Stability, Lateral and Directional - Dynamic (1.8.1.2.2)
5. Flying Qualities (1.8.5)
6. Mass and Gyroscopic Problems (1.8.6)
7. Loads, Maneuvering - Wings (4.1.1.1.2)
8. Loads, Maneuvering - Tail (4.1.1.2.2)

(over)

[redacted]

NACA RM H55A13

Copies obtainable from NACA, Washington

NACA RM H55A13

CONFIDENTIAL

9. Loads - Fuselage, Nacelles, and Canopies (4. 1. 1. 3)
I. NACA RM H55A13

NACA

CONFIDENTIAL

NACA RM H55A13

Copies obtainable from NACA, Washington

NACA RM H55A13

CONFIDENTIAL

9. Loads - Fuselage, Nacelles, and Canopies (4. 1. 1. 3)
I. NACA RM H55A13

NACA

CONFIDENTIAL

NACA RM H55A13

Copies obtainable from NACA, Washington

NACA RM H55A13

CONFIDENTIAL

9. Loads - Fuselage, Nacelles, and Canopies (4. 1. 1. 3)
I. NACA RM H55A13

NACA

CONFIDENTIAL

Copies obtainable from NACA, Washington

NACA

CONFIDENTIAL